Environ Earth Sci (2015) 73:39–55
DOI 10.1007/s12665-014-3393-4

ORIGINAL ARTICLE

A hydrogeochemistry and isotopic approach for the assessment of surface water–groundwater dynamics in an arid basin: the Limarí watershed, North-Central Chile

Ricardo Oyarzún · Elizabeth Jofré · Paulina Morales · Hugo Maturana · Jorge Oyarzún · Nicole Kretschmer · Evelyn Aguirre · Patricio Gallardo · Luis E. Toro · José F. Muñoz · Ramón Aravena

Received: 7 April 2013 / Accepted: 27 May 2014 / Published online: 11 June 2014

Abstract This paper describes the results of a hydrochemistry and isotopic study of surface water and groundwater dynamics at the Limarí River basin, arid North-Central Chile. The study involved two sampling campaigns, performed in April (Fall, at the end of the irrigation season) and December 2010 (late Spring, at the peak of the irrigation season). The main results show the effect of La Paloma and Hurtado dams on the chemical and isotopic compositions of the Grande and Hurtado rivers (main tributaries of the Limarí River), the influence of return flows to the Limarí River from surface water irrigation in agricultural areas, the local effects of metallurgical operations in the El Ingenio Creek, the effect of water–rock interaction processes, and the nearby coastal belt influence on the Punitaqui Creek area and the lower part of the Limarí River. In addition, this study shows an active interaction between surface water and shallow groundwater, and a minor importance of local precipitation events, on the hydrological behavior in the study area. An exception is the Rinconada de Punitaqui zone where the results are consistent with the origin of the water being associated with local precipitation. Also, sources of sulfate, which is present in high levels especially in surface waters, have been assessed. The results of this study, based on an integrated use of chemical and isotopic tracers, provide sound and useful information to establish the level of interaction between surface water and groundwater, allowing the development of a hydrological conceptual model for the area.

Keywords Environmental isotopes · River−aquifer interaction · Flow conceptual model

R. Oyarzún (✉) · H. Maturana · J. Oyarzún
Departamento Ingeniería de Minas, Universidad de La Serena, Benavente 980, La Serena, Chile
e-mail: royarzun@userena.cl

R. Oyarzún · N. Kretschmer
Centro de Estudios Avanzados en Zonas Aridas, La Serena, Chile

E. Jofré · P. Morales
Ingeniería Civil Ambiental, Universidad de La Serena, La Serena, Chile

E. Aguirre · P. Gallardo
Comisión Chilena de Energía Nuclear, Santiago, Chile

L. E. Toro
Isotope Hydrology Section, International Atomic Energy Agency, Vienna, Austria

J. F. Muñoz
Departamento Ingeniería Hidráulica y Ambiental, Pontificia Universidad Católica de Chile, Santiago, Chile

R. Aravena
Department of Earth and Environmental Sciences, University of Waterloo, Waterloo, Canada

Introduction

Arid and semi-arid zones, i.e., areas where the ratio of annual precipitation (P) to potential evapotranspiration (ETp) is lower than 0.5 (Maliva and Missimer 2012), extent for over 30 % of the earth's surface, and are typically found between latitudes 15°–35°, both northern and southern hemisphere (Simmers 2003; Herczeg and Leaney 2011). An increased demand for water on these hydrologically fragile zones is already occurring worldwide, due to factors such as population growth and economic development based on water demanding activities such as agriculture and mining. In addition to this increased demand,

there is a threat of water shortage due to climate change effects (Shi et al. 2001; CONAMA 2006; Souvignet et al. 2010). This is a common situation at several basins in North-Central Chile, such as the Limarí River watershed, which is the subject of this work.

In order to cope with these issues, the adoption of integrated water resources management strategies is essential. This requires proper knowledge of different water resources or components of the hydrological cycle, as well as of the processes affecting water composition, under a holistic and sustainable approach. At the basin scale, the use of environmental tracers emerge as a suitable and relatively easy-to-use approach, in particular for a preliminary assessment in places where there is a lack of basic knowledge on water quality and on the relations and dynamics of surface water–groundwater interactions (SW–GW) (Baskaran et al. 2009). Tracers typically used include, among others, (a) common dissolved water constituents, such as major cations and anions, and (b) water stable isotopes of oxygen (^{18}O) and hydrogen (^{2}H).

The chemical composition of surface water and groundwater is controlled by several interrelated factors, a major one being water–rock interaction, which in most unpolluted catchments is the dominant source of solutes (Drever 1997). Other important factors are related to climate, in terms of temperatures (solubility-temperatures relations) and precipitation, mix of waters, relief, vegetation, time, and local geology, as natural acid drainage is a major source of SO_4^{2-}, H^+, and sulphophile metals. Finally, anthropogenic activities may also greatly affect chemical and physical water properties (Freeze and Cherry 1979; Drever 1997; Shi et al. 2001; Güller et al. 2002). Thus, the spatial and temporal variability in the abundance of ions in water can provide insight on the main physical and chemical processes controlling water chemistry, aquifer heterogeneity, and SW–GW connectivity characteristics (Thyne et al. 2004; Matter et al. 2005; Demirel and Güller 2006). Likewise, environmental isotopes such as deuterium and oxygen-18 are used in hydrologic sciences for water characterization and the identification of different water sources in hydrologic and hydrogeologic systems given that (a) they constitute the water molecule, and (b) they experiment a fractionation process throughout the hydrological cycle, as determined by evaporation and precipitation processes (Clark and Fritz 1997; Mook 2001). Thus, they become important water management tools (e.g., Guay et al. 2006).

Agriculture is by far the largest water demanding activity for consumptive use in Chile (Oyarzún et al. 2008), with ca. 75 % of the country's total water use. In arid to semiarid North-Central Chile (18°30′–32°15′S latitude), the Coquimbo Region is by far the region with the most important agricultural activity, and within the Coquimbo Region, the Limarí basin is the most important agricultural area, where a sustained increase in irrigated area through the years has occurred. This situation, as well as the introduction of new permanently water demanding crops such as avocado and sweet orange, has further modified seasonal water consumption patterns and added additional stress on the limited water resources. This motivated the official declaration of Limarí in 2005 by the Chilean Water Authority (Dirección General de Aguas, DGA), as an "over allocated" catchment (DGA 2008). The practical significance of this statement is that no new permanent consumptive surface water right can be granted in the basin. Therefore, groundwater resources have become susceptible to increased demand and use, generating a conflictive situation when groundwater is extracted from shallow wells in the alluvial plain near the streams. Although groundwater and surface water are legally two different resources in Chile, they normally interact and disputes between water users due to SW–GW interaction issues have reached civil suit status (Alvarez and Oyarzún 2006). Moreover, as more recently recognized by the DGA (Dirección General de Aguas) (2008), "in general, in the Limarí basin there is very limited information on the degree of interaction between rivers and aquifers." Finally, while there is a rather comprehensive monitoring network of surface water quality managed by DGA (Espejo et al. 2011), little attention has been granted to the geochemistry of groundwater in this important and sensitive area, and therefore information about groundwater quality is rather scarce in the Limarí basin, both in space and in time (Strauch et al. 2009).

The main objectives of this contribution are twofold: first, to characterize the chemical and isotopic composition of surface waters and shallow groundwater in the Limarí river basin and to gain insight about the main factors and processes that influence them; and second, to perform a preliminary assessment on the SW–GW relationship in the studied area. It is envisioned that a proper and integrated knowledge of surface waters and groundwater geochemistry will contribute to a more efficient water management in this area.

Study area

The Limarí basin is located between 30°20′–31°15′S latitude and 70°30′–71°49′W longitude, in the arid to semiarid Coquimbo Region, North-Central Chile. This study focuses on the lower part of the catchment, downstream from the La Paloma (750 Hm^3, located at 350 masl) and Recoleta (100 Hm^3, located at 370 masl) water reservoirs (Fig. 1).

Climate is characterized by frequent cloudy conditions, mild temperature and humidity, with an annual rainfall

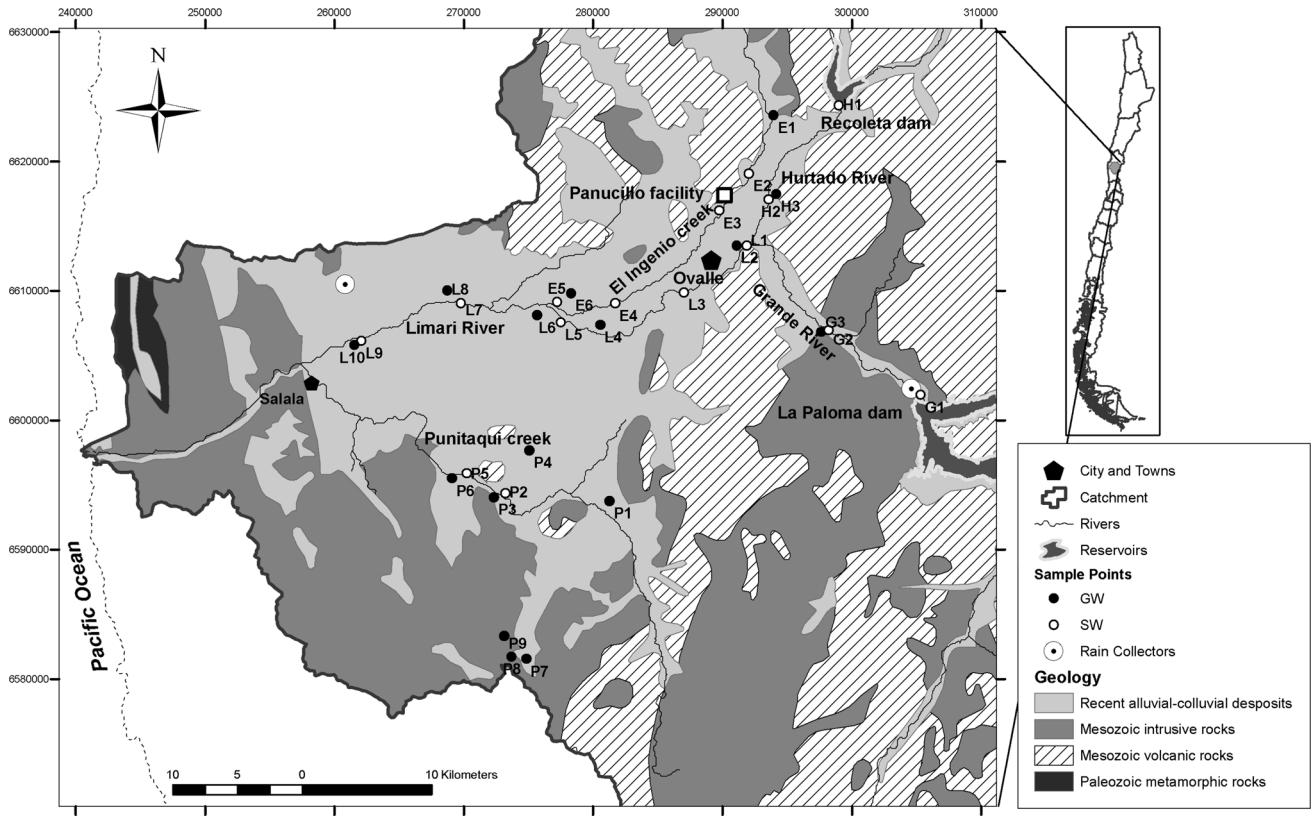

Fig. 1 Major geological formations and locations of the sampling points for the study area

average of 130 mm (concentrated from mid June to mid September), an annual potential evapotranspiration over 1,200 mm, and a dry period of 8–9 months. There is no snowfall in the study area. Annual average temperature is 16 °C, with a daily average minimum and maximum of 9 °C (July) and 24 °C (January) (DGA 2004).

The Limarí River is formed by the confluence of the Grande and Hurtado rivers, located at an altitude of ca. 230 masl, 4 km upstream from Ovalle, the main city in the catchment (population of ca. 100,000 inhabitants). From the confluence of the Hurtado and Grande rivers, the watercourse is named Limarí, which after 60 km reaches the Pacific Ocean. Although variable in space and time, the average flows of the rivers Grande, Hurtado and Limarí are around 3.9, 1.2, and 2.3 m^3/s, respectively (DGA 2004). Given that the flows of the Hurtado and Grande rivers are regulated by the Recoleta and Paloma dams, respectively, discharge downstream from the dams rarely represents the concurrent inflows to the reservoirs. Moreover, the dams' deliveries to the rivers, as well as river water diversions (irrigation channels) reach their peak in the irrigation season between November and March. Between Ovalle and the Limarí River outlet, the river receives two tributaries with low importance in term of discharge but relevant in terms of water quality: El Ingenio and Punitaqui creeks. Both of them originate in the Coastal Cordillera zone, corresponding to rather small sub-basins with maximum elevations of ca. 950 and 850 masl, respectively (DGA 2004).

The existence of the La Paloma and Recoleta reservoirs (as well a third one, Cogotí, outside the studied area), as well as the use of modern water application techniques (drip and trickle irrigation) sustain an important agricultural activity with ca. 20,000 ha of permanent crops as well as a similar extension of irrigated grasslands (INE 2007).

The general geological traits of the Limarí basin were established by the classic publication of Thomas (1967), presented at a 1:250,000 scale. Most recent studies, like that of Emparán and Pineda (2006), presented at a 1:100,000 scale, have provided new geological details and important radiometric age data on parts of the basin. The dominant volcanic–plutonic geological setting of the Limarí River basin expresses the almost continuous Mesozoic–Cenozoic generation of calc-alkaline magmas, a consequence of the subduction of Pacific oceanic tectonic plates under the western edge of the Continent. Among the plutonic rocks, granodioritic composition is dominant, whereas basaltic andesitic composition is frequent in volcanic flows and andesitic to dacitic lithologies are common in pyroclasts and clastic sedimentary beds intercalated in

the volcanic series. Main minerals are pyroxene, amphibole, and Ca–Na plagioclase. Average MgO, CaO, Na_2O, and K_2O contents are (in %) 3.8, 8.1, 3.7, 1.2 for andesites, and 1.7, 4.6, 4.2, 2.0 for granitic rocks (López-Escobar et al. 1979; Oyarzún et al. 1993). The age of the rocks is mainly Cretaceous in the central part of the basin whereas Jurassic volcanic-sedimentary series and batholitic rocks of this age crop out both on its eastern Andean part, as well as on its western coastal flank, together with Paleozoic intrusive and metamorphic rocks.

Rock weathering, especially the chemical one, is generally weak, both on the Andean range and in that part of the catchment considered in the current study. Aridity, coupled with step topography in the Andes (e.g., the Grande river runs down from the higher peaks at 4,870 masl to La Paloma water reservoir at 350 masl in only 70 km) are responsible for a strong dominance of physical over chemical weathering. However, a large number hydrothermal alteration zones linked to partly oxidized sulphide minerals are an important source of SO_4^{2-}, Na^+, Ca^{2+}, and Mg^{2+}, supplied to the drainage by the altered, mainly igneous, calc-alkaline rocks. In addition, the outcrops of granitic rocks present some degree of chemical weathering due to its "granular" structure that facilitates the breaking up of its minerals.

Because of the igneous origin of most of these rocks, its permeability is largely secondary and mainly restricted to fracturing in fault zones. East from 71°15′ (approximately where Ovalle is located), alluvial sediments are restricted to the narrow plains of the steep tributary rivers. However, west of 71°15′, the Limarí River exhibits a wider alluvial plain and Pliocene to Quaternary fluvial and partly marine terraces cover an important part of the basin. From Ovalle to the town of Salala, where the alluvial sedimentary deposits attain its maximum depth, only the upper aquifer unit (about 20 m thick) attains favorable characteristics, i.e., hydraulic conductivities in 10^{-4} to 10^{-2} m/s range. (SERPLAC et al. 1979; Espinoza 2005).

Methodology

Two sampling campaigns were performed in this study: one in April 2010 (Fall, at the end of the irrigation season), and one in December 2010 (late Spring, at the peak of the irrigation season). In both campaigns, 15 samples of surface water (SW) and 16 of groundwater (GW) were collected. The sampling points are located in the area of the Grande (3), Hurtado (3), and Limarí (10) rivers and in the areas of the El Ingenio (6) and Punitaqui (9) creeks (Fig. 1). The selection of the surface water locations was based on proximity to the groundwater sampling wells. Regarding the latter, most are shallow wells (normally less than 30 m depth) that provide drinking water to local rural communities ("Agua Potable Rural", APR). Prior to groundwater sampling, wells were purged of a volume of water equivalent to three times the volume of the well casing and/or until field parameters stabilized (ca. 5 min pumping). The exception corresponds to groundwater samples taken in the Rinconada de Punitaqui area (P7, P8, P9), which collected from shallow hand-dug wells and springs, which are continuously used by the local rural community.

At each sampling location, two 1-L bottles were filled. One of them was acidified (HNO_3, 2 % v/v) and used for cations and trace elements determinations, and the second, not acidified, was used for anions determinations. A Hanna HI982804 multiparameter probe was used for field physico-chemical determinations of total dissolved solids (TDS), electrical conductivity (EC), dissolved oxygen (DO), and pH. Samples were kept refrigerated (ca. 4 °C) during field campaigns. Also, additional samples for isotope analysis were obtained in 125-ml plastic bottles following the recommendations of the International Atomic Energy Agency (Aggarwal et al. 2007).

Samples were analyzed at laboratories of the Chilean Nuclear Energy Commission (CCHEN) in Santiago. Chemical analyses were performed on filtered (0.45 μm) samples following the procedures established in Standard Methods, 20th edition (Clesceri et al. 1999). ICP Optic emission spectrometry was used for P, Li, Na^+, Al, Fe, Mn, Pb, Zn, As, Cd, Cu, K^+, Ca^{2+}, Mg^{2+}; high precision liquid chromatography (HPLC) for Cl^-, SO_4^{2-} and NO_3^-; and potentiometric titration for HCO_3^-. Detection limits, in mg/l were: 0.1 for P, Li, Al, Fe, Mn, Pb, Zn, Cl^-, SO_4^{2-}, K^+; 0.25 for NO_3^-; 0.02 for As, Cd, and Cu; 1 for Na^+, Ca^{2+} and Mg^{2+}; and 20 for HCO_3^-. Isotopic determination of oxygen and deuterium were performed at the Environmental Isotope Laboratory of CCHEN, using a Liquid Water Stable Isotope Analyzer (Los Gatos Research). The instrument uses off-axis integrated cavity output spectroscopy to measure absolute abundances of ^2HHO, $HH^{18}O$ and HHO via laser absorption.

Rainfall water samples were obtained during 2009 and 2010 at three collectors installed both within and upstream of the study area, at Carretera (214 masl), La Paloma Dam (335 masl) and Tulahuén (Grande River, upstream from La Paloma, 987 masl) stations. Water samples were collected on a rainfall event-base (3 events each year), and the isotope data were weighted by the rainfall amount of each event, to obtain a representative local meteoric line (Friedman et al. 1992).

Also, based on the chemical results obtained in the first sampling campaign, as well as due to concerns raised by local water users and basin stakeholders, additional samples were considered for the second sampling campaign

(December). These additional samples were also analyzed for sulfate isotopes ($\delta^{34}S–SO_4^{2-}$ and $\delta^{18}O–SO_4^{2-}$), in order to identify the sources of sulfate in waters (Clark and Fritz 1997). $BaSO_4$ precipitates, obtained by $BaCl_2$ addition to the samples, along with a few ml of the original water samples were sent for isotope analysis to the Environmental Isotope Laboratory at the University of Waterloo, Canada. At the laboratory, purified $BaSO_4$ was weighed in a tin capsule along with Nb_2O_5 and combusted at 1,000 °C in a Costech EA to produce SO_2, which was carried in a helium stream to a Micromass IsoChrom-IRMS where it was analyzed (Morrison et al. 1996). In addition, the purified $BaSO_4$ was combusted in a HEKAtech 1,350 °C Pyrolysis furnace to produce CO, which was then carried in a helium stream to a GVI IsoPrime-IRMS where it was analyzed for ^{18}O (Morrison 1997). The precisions for the sulfate isotope determination were 0.3 ‰ for ^{34}S and 0.5 ‰ for ^{18}O.

Isotope ratios are expressed in per mil (‰) using the usual δ notation, relative to the V-SMOW standard for oxygen and hydrogen isotopes, and the international standard Canyon Diablo Troillite (V-CDT) for sulfur isotopes. Thus, δ (‰) = (Rsample/Rstandard – 1) × 1,000, where R stands for $^{18}O/^{16}O$, $^{2}H/^{1}H$, or $^{34}S/^{32}S$. Finally, the deuterium excess, i.e., d-excess = $\delta^2H - 8\delta^{18}O$ (Dansgaard 1964; Carreira et al. 2011; Yin et al. 2011), was determined.

Results and discussion

Spatial and temporal variations in water chemistry

Physicochemical and isotope characteristics of surface water and groundwater are listed in Table 1. According to sampling location, type, and sampling timing, samples were divided into five groups: Hurtado (H), Grande (G), El Ingenio (E), Punitaqui (P), and Limarí (L), April and December, and into surface waters and groundwater. Nitrate exhibited very low concentrations (the average of the samples were ca. 1.6 and 4 mg/l of $N–NO_3$ for surface waters and groundwater, respectively), whereas trace elements (P, Al, Fe, Mn, Pb, Zn, As, Cd, Cu, and Li) in general yielded values below detection limits; therefore, all these parameters were excluded from Table 1 and are not part of the following data analysis. Furthermore, no major differences were observed between the results of both sampling campaigns. Thus, the following spatial–temporal analysis is based on the second sampling results (although it is addressed when some changes in water composition were detected) considering that December is the period when the water is most used in the basin (especially for irrigation purposes), and therefore, when water diversion (through irrigation channels) and water application (crop irrigation) could be of greater importance in terms of influencing the dynamics of surface water–groundwater relationship.

In general, waters exhibit a neutral to slightly alkaline pH (Table 1). Regarding the EC, the higher values in surface waters are found at the El Ingenio Creek, and in the lower part of the studied area (L7 and L9, Table 1). A similar pattern is found for groundwater (in both campaigns), especially in the lower part of the study area (locations L8 and L10).

Surface waters and groundwater evolved (in the direction of the flow) from $Ca–HCO_3$ in the upper zone (e.g., G1, G2, G3, H1, H2, H3, L1, L2, and L3 sample locations) to mixed Ca–Na–Cl water types in the lower part of the studied area, especially after the confluence of the Limarí River with El Ingenio Creek (e.g., from L7 to L10) (Fig. 2). The spatial evolution of this pattern, as well as the increase in salinity throughout the studied area, is verified from the Stiff diagrams shown in Fig. 3. This pattern could be associated to greater evaporation in the lower part of the region, but can also be partly associated to input of salts from evaporative-derived materials present in the marine terraces, which can explain the relative high concentration of Ca^{2+}, Cl^-, and SO_4^{2-} in these waters.

An interesting exception to this general situation is the El Ingenio Creek surface water sample at E3, which is $Ca–SO_4$ type water, very likely as a consequence of input from a recently closed Panulcillo mining plant, an important source of sulfate pollution, associated to the leaching of sulfide minerals, which is located upstream of that sampling point. Despite the fact that Panulcillo ended metallurgical operations by 2010, its effects on water quality, especially surface water, remain relevant for El Ingenio Creek. Surface water in the lower part of the Ingenio Creek basin (E4, E5), similarly than the Limarí River, can also be influenced by input of salts from evaporative-derived materials present in the marine terraces. This aspect is further discussed in the section sulphur isotopes.

Figures 2 and 3 also includes the sampling locations P7 and P9, which are hand-dug wells and tunnels ("galerias filtrantes", kind of small qanat) that intercept the aquifer in the non-irrigated (dry) land area of the Rinconada de Punitaqui sub-basin, which is not part of the main river flow and irrigation channel network where all the other sampling stations are located. It can be observed that these locations, despite being close to the Limarí basin outlet, present a different hydrochemical imprint, even distinct from those of the Punitaqui Creek area (P1 to P6). Indeed, the Rinconada de Punitaqui samples are classified as Na-HCO_3 (P7) and Ca-HCO_3 (P9) waters, with the lowest ion contents of all the groundwater sampled in the area of study (EC between 433 and 692 μS/cm).

Table 1 Chemical and isotopic composition of surface waters and groundwaters in the area of study

Season	Component	ID	pH	EC (uS/cm)	TDS (mg/L)	Na^+ (mg/L)	K^+ (mg/L)	Ca^{2+} (mg/L)	Mg^{2+} (mg/L)	Cl^- (mg/L)	HCO_3^- (mg/L)	SO_4^{2-} (mg/L)	δ^2H (‰)	$\delta^{18}O$ (‰)	d-excess (‰)	$\delta^{18}O$ (SO_4) (‰)	$\delta^{34}S$ (SO_4) (‰)
April	Surface water	H1	7.7	462	271								−68.6	−8.09	−3.9		
		H2	7.6	750	441	46.6	2.4	106.0	20.8	32.5	223	157	−73.9	−9.30	0.5		
		G1	7.9	336	187	19.7	1.9	35.9	9.9	9.7	120	52	−60.6	−7.17	−3.2		
		G2	8.1	386	216	20.3	1.9	45.0	11.3	11.6	153	47	−61.5	−7.36	−2.6		
		E2	7.6	872	488	84.7	3.7	63.4	42.8	76.6	331	111	−68.0	−8.62	1.0		
		E3	7.8	2,056	1,377	121.0	7.7	244.0	118.0	138.0	233	964	−63.9	−7.93	−0.5		
		E4	7.8	3,061	1,799	330.0	7.1	219.0	124.0	521.0	370	535	−59.8	−7.45	−0.2		
		E5	7.9	2,677	1,562	292.0	7.0	202.0	99.0	519.0	321	420	−59.2	−7.39	−0.1		
		P2	8.1	1,482	827								−47.6	−6.28	2.6		
		P5	8.1	2,163	1,201	159.0	6.6	110.0	59.6	363.0	369	277	−45.8	−5.86	1.1		
		L1	8.1	512	288	43.3	2.6	61.0	16.2	22.9	199	66.4	−62.2	−7.69	−0.7		
		L3	7.9	591	333	63.8	1.9	55.2	15.1	29.1	209	81	−62.0	−7.72	−0.2		
		L5	8.9	1,036	593	117.0	6.3	98.2	23.6	115.0	237	135	−60.5	−7.44	−1.0		
		L7	8.3	2,014	1,142	238.0	6.8	155.0	57.5	365.0	254	259	−58.6	−7.06	−2.1		
		L9	7.8	2,357	1,327	292.0	8.1	168.0	71.0	472.0	259	281	−55.1	−6.71	−1.4		
	Groundwater	H3	6.9	708	410	37.4	2.3	95.8	16.9	29.2	225	142	−75.4	−9.50	0.6		
		G3	7.1	582	327	35.6	2.1	69.4	15.9	19.2	237	68	−63.6	−8.04	0.7		
		E1	7.1	856	495	77.1	5.2	55.6	41.9	57.5	286	146	−57.3	−7.47	2.5		
		E6	7.1	1,768	1,019	187.0	4.3	153.0	53.0	281.0	369	245	−59.7	−7.38	−0.7		
		P1	7.6	1,113	614	114.0	2.2	64.4	39.1	157.0	270	139	−52.8	−6.84	1.9		
		P3	7.8	1,345	749	129.0	3.2	95.3	51.9	177.0	360	141	−45.6	−5.94	1.9		
		P4	7.8	2,015	1,160	263.0	3.5	128.0	46.6	307.0	266	325	−54.5	−7.05	1.9		
		P6	7.7	1,789	998	194.0	5.1	131.0	79.5	263.0	400	185	−44.6	−5.64	0.5		
		P7	7.4	515	277	51.2	2.0	25.4	21.4	40.7	212	19	−35.4	−5.90	11.8		
		P8	7.5	692	374								−35.9	−5.86	11.0		
		P9	7.6	536	299	40.5	3.1	38.5	23.2	30.2	223	13	−34.7	−5.89	12.4		
		L2	7.3	744	416	60.8	2.2	82.2	18.5	43.5	246	116	−66.3	−8.26	−0.2		
		L4	7.2	941	537	89.4	3.7	96.0	22.9	58.3	318	142	−62.9	−7.75	−0.9		
		L6	7.5	1,730	985	203.0	5.0	171.5	34.0	251.0	361	256	−60.3	−7.65	0.9		
		L8	7.2	3,221	1,799	323.0	7.4	251.0	115.0	681.0	516	370	−55.2	−6.82	−0.6		
		L10	8.0	2,502	1,431	265.0	7.3	194.0	73.0	465.0	317	331	−55.3	−6.66	−2.0		
December	Surface water	H1	9.0	481	225	23.0	2.5	76.2	13.8	12.0	161	111	−68.9	−8.22	−3.1	3.03	4.86
		H2	8.7	739	341	39.8	1.9	113.0	20.2	43.3	242	147	−75.5	−9.61	1.4	3.82	5.82
		G1	8.7	364	170	21.3	2.0	49.8	12.3	10.2	159	52	−63.4	−7.97	0.4	3.59	4.12

Table 1 continued

Season	Component	ID	pH	EC (uS/cm)	TDS (mg/L)	Na^+ (mg/L)	K^+ (mg/L)	Ca^{2+} (mg/L)	Mg^{2+} (mg/L)	Cl^- (mg/L)	HCO_3^- (mg/L)	SO_4^{2-} (mg/L)	δ^2H (‰)	$\delta^{18}O$ (‰)	d-excess (‰)	$\delta^{18}O$ (SO_4) (‰)	$\delta^{34}S$ (SO_4) (‰)
		G2	8.8	379	178	23.0	1.9	54.4	13.0	12.8	171	57	−62.5	−7.56	−2.0	4.49	5.06
		E2	8.5	858	398	84.7	2.8	70.7	40.7	78.7	326	119	−64.4	−8.26	1.7	7.44	9.04
		E3	7.6	1,870	864	114.0	3.1	266.0	85.9	151.0	270	767	−61.7	−7.53	−1.5	9.15	0.79
		E4	7.9	2,957	1,496	322.0	6.2	241.0	125.0	557.0	419	507	−59.4	−7.41	−0.1	10.08	14.68
		E5	8.1	2,681	1,306	275.0	6.3	211.0	97.7	545.0	376	393	−58.9	−7.32	−0.3	8.66	13.13
		P2	8.3	1,443	677	162.0	4.9	103.0	64.0	212.0	416	174	−43.8	−5.60	1.0	9.64	14.05
		P5	8.1	2,614	1,266	307.0	7.5	168.0	102.0	498.0	469	342	−42.6	−5.28	−0.4	9.99	17.87
		L1	8.8	519	243	38.8	2.0	67.0	15.7	22.6	227	72	−61.2	−7.49	−1.3	6.11	6.89
		L3	8.9	534	269	50.5	2.1	66.8	16.3	28.4	229	80	−61.6	−7.55	−1.2	6.74	6.81
		L5	8.2	1,166	547	134.0	5.3	117.0	26.0	157.0	321	159	−58.8	−7.33	−0.2	7.72	12.90
		L7	8.1	2,392	1,240	278.0	6.6	199.0	77.0	550.0	299	328	−56.4	−6.96	−0.7	9.65	15.98
		L9	8.3	2,482	1,292	286.0	6.8	198.0	81.8	569.0	288	321	−54.2	−6.58	−1.6	10.68	15.92
	Groundwater	H3	7.7	694	323	35.7	1.9	113.0	18.7	37.6	232	143	−74.7	−9.52	1.5	3.59	5.26
		G3	7.8	608	291	40.8	2.3	92.0	19.6	26.1	297	86	−62.9	−8.06	1.6	9.20	7.96
		E1	8.1	1,791	374	75.4	4.2	60.7	42.5	59.2	272	131	−56.7	−7.59	4.0	4.84	5.14
		E6	7.5	2,199	1,078	221.0	5.7	197.0	72.1	394.0	417	299	−59.0	−7.31	−0.5	11.45	14.92
		P1	7.4	1,232	589	146.0	3.2	69.4	40.4	146.0	318	131	−55.2	−7.09	1.5	5.59	12.66
		P3	7.5	1,253	585	136.0	3.9	106.0	56.0	173.0	422	135	−47.0	−6.17	2.4	10.93	13.97
		P4	7.7	1,920	950	264.0	4.4	140.0	48.2	317.0	310	311	−53.9	−7.04	2.4	6.65	13.38
		P6	7.6	2,087	1,041	245.0	6.2	149.0	89.8	374.0	492	252	−44.4	−5.50	−0.4	10.47	16.78
		P7	7.0	487	225	52.4	2.5	32.0	26.1	37.5	226	16	−35.1	−5.82	11.5	4.52	10.92
		P8	7.4	687	320								−35.6	−5.96	12.1	5.04	9.50
		P9	8.0	434	204	32.9	4.1	36.9	21.0	30.0	190	11	−34.5	−5.90	12.7	2.91	9.07
		L2	8.1	850	301	54.0	2.5	85.2	17.7	40.8	253	99	−63.7	−7.95	−0.1	6.41	6.85
		L4	7.3	898	440	94.8	3.5	108.0	25.1	68.0	377	119	−62.7	−7.63	−1.7	7.37	9.86
		L6	7.7	2,248	677	162.0	3.9	154.0	30.5	213.0	387	204	−59.7	−7.56	0.8	9.43	14.57
		L8	7.9	3,549	1,696	339.0	8.5	281.0	126.0	805.0	392	417	−54.0	−6.60	−1.2	10.25	15.26
		L10	7.3	2,690	1,256	288.0	7.9	227.0	85.6	598.0	353	327	−54.3	−6.63	−1.3	10.83	16.07

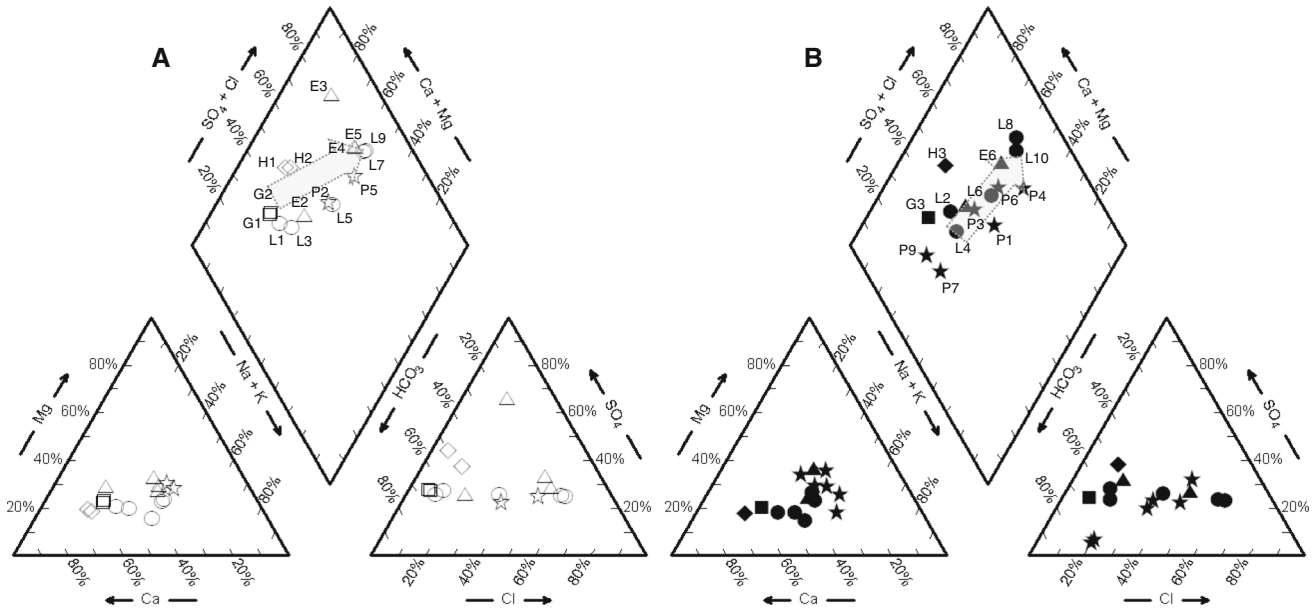

Fig. 2 Piper diagrams for surface waters (**a**) and groundwater (**b**)

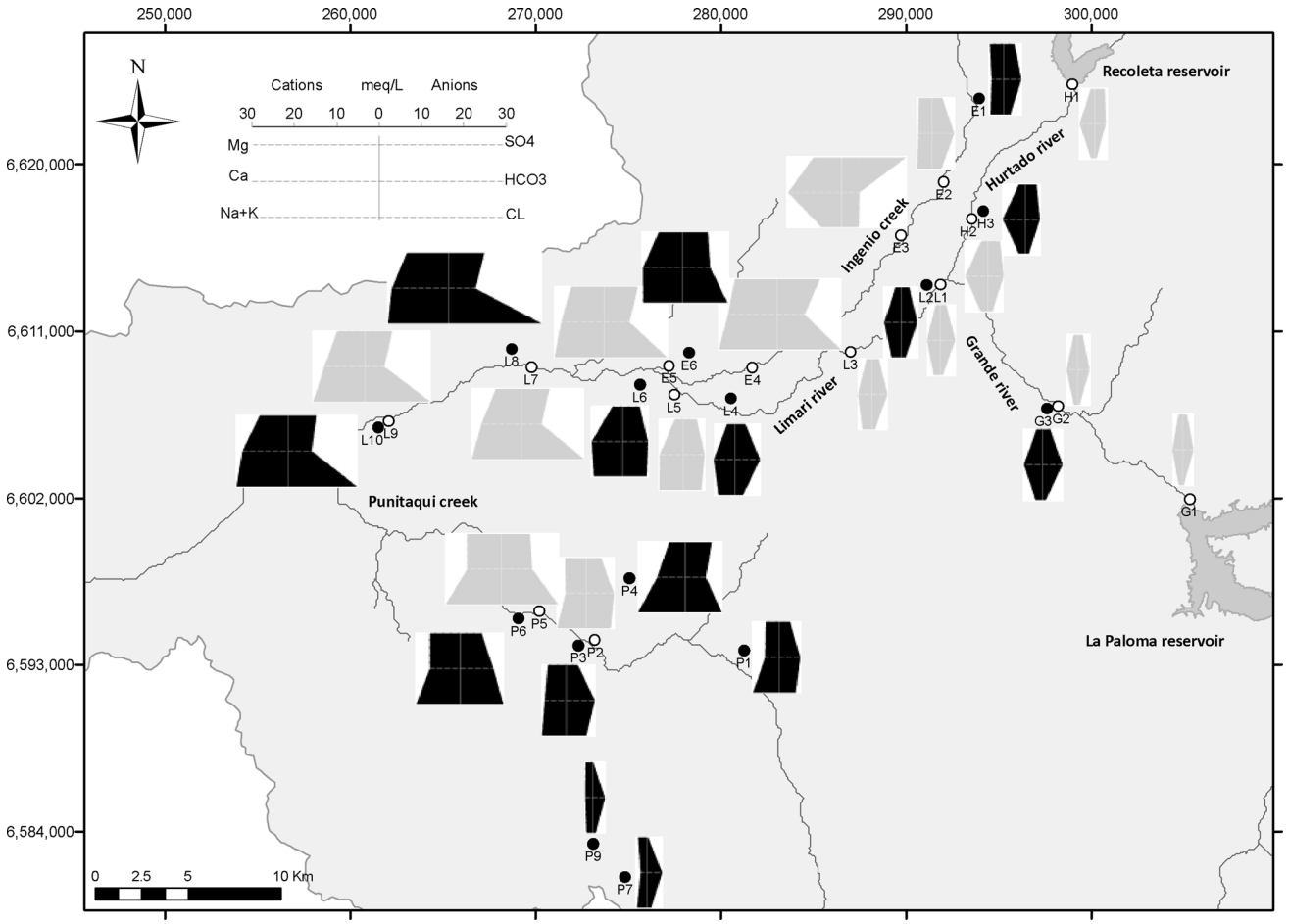

Fig. 3 Stiff diagrams for surface waters (*light gray shapes*) and groundwater (*black polygons*) for the December sampling campaign

Finally, the hydrochemical information shows that surface waters and groundwater in neighboring locations (e.g., G2-G3, L4-L5, P2-P3, L9-L10, and so on) exhibit rather similar chemical compositions, which is considered important evidence of an active local SW–GW interaction. This is shown clearly in Fig. 4, which presents TDS, Na^+, Ca^{2+}, Mg^{2+}, Cl^-, HCO_3^-, SO_4^{2-} variations throughout an E-W profile following the Grande and Limarí rivers. Also, a clear change is evident from sample L7, which coincides with the widening of the floodplain, and greater accumulation of alluvial deposits, which likely favor evaporation processes (as the river increases its sinuosity and water flow slower) and greater groundwater-aquifer sediments interaction. Finally, both Cl^- and Ca^{2+} patterns depart from Na^+ and SO_4^{2-} respectively, exhibiting a strong increase in their relative concentrations in the lower part of the basin. The input of salts from the marine terraces can explain part of this trend in the lower part of the basin. The role of evaporation will be explored further analyzing the isotope data in water samples.

Sources of major components

The main processes determining water chemistry were assessed using Gibbs and van Wirdum diagrams. As shown in Yang et al. (2012) and Xiao et al. (2012), the Gibbs diagram represents a meaningful tool to assess the relative importance of three major processes (i.e., atmospheric precipitation, rock weathering, and evaporation) over water chemistry. Thus, as shown in Fig. 5, mainly rock-dominant processes (i.e., water–rock interaction), and evaporation events to a lesser extent, appear to control both surface water and groundwater composition in the study area. It is also of interest to observe that, especially in the anion related diagram, a sort of water evolution path arises. Indeed, as shown in the figures, the cluster with lower total dissolved solids (in the field of rock weathering dominance but closest to the precipitation field when compared with the other clusters) is the one formed by the samples taken at the initial section (i.e., upstream) of the study area. On the other side, the cluster that lies in the evaporation dominance field corresponds to those samples taken at the end of the El Ingenio creek and Limarí river (E4, E5, E6, L7, L8, L9, L10, P4, P5, P6), i.e., water that have being under evaporative conditions for a longer period (this is also the case in the cation-related diagram, Panel A). Part of the trends observed in Fig. 5 can also be explained by water-sediments interaction in the area of marine terraces located in the lower part of the basin, in case of the Limarí River, and input of high salinity groundwater in case of the Ingenio Creek. In order to constrain the types of water–rock interactions, the Ca^{2+}/Na^+, Mg^{2+}/Na^+, and HCO_3^-/Na^+ ratios can be used (Xiao et al. 2012). Indeed, for carbonate weathering these ratios are close to 50, 10, and 120, whereas for silicate weathering these values are close to 0.35, 0.24, and 2, respectively (Gaillardet et al. 1999; Xiao et al. 2012). As shown in Table 2, for the Limarí River basin, the obtained values point toward the latter process as

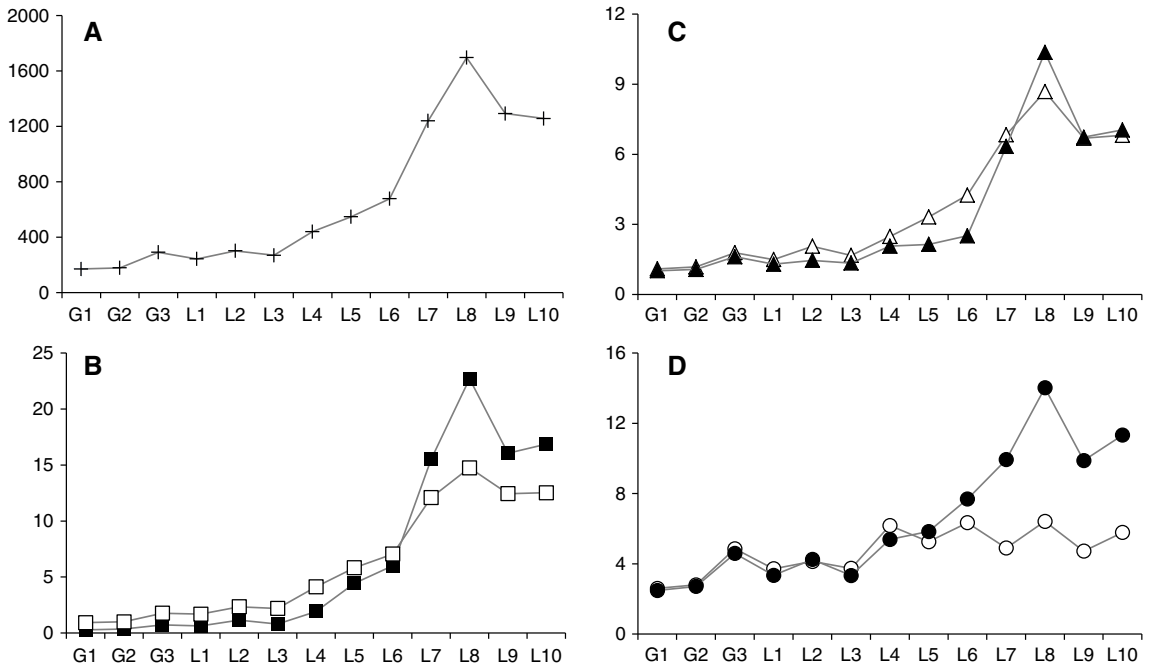

Fig. 4 Flow path profiles of total dissolved solids (mg/l) and selected cations and anions (meq/l). **a** Total dissolved solids; **b** Na^+ (*open square*) and Cl^- (*filled square*); **c** Mg^{2+} (*filled triangle*), and SO_4^{2-} (*open triangle*); **d** Ca^{2+} (*filled circle*) and HCO_3^- (*open circle*)

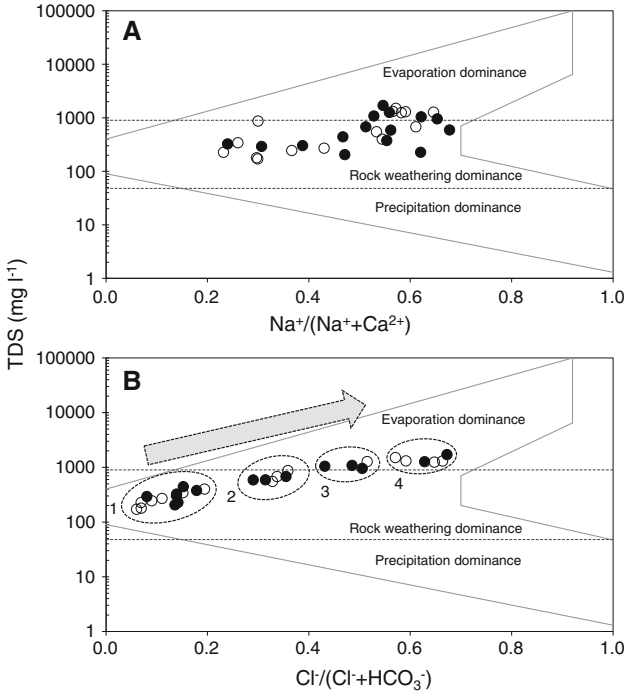

Fig. 5 Gibbs diagrams illustrating the most likely controlling mechanism of water chemistry in the study area (*open circle* surface waters; *filled circle* groundwaters). Cluster 1: H1, H2, H3, G1, G2, G3, E1, E2, L1, L2, L3, L4, P7, P9; Cluster 2: E3, L5, L6, P1, P2, P3; Cluster 3: P4, P5, P6, E6; Cluster 4: E4, E5, L7, L8, L9, L10

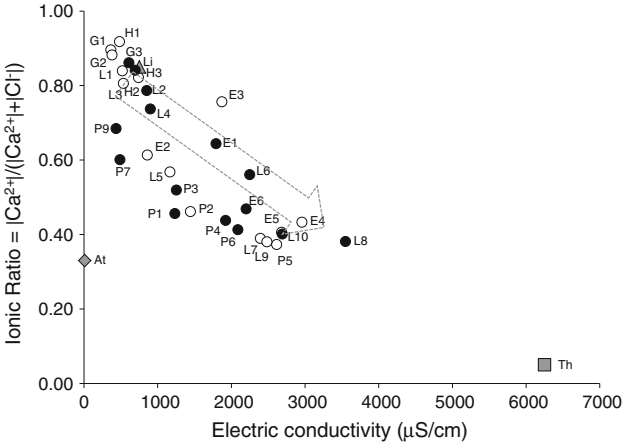

Fig. 6 Van Wirdum's diagram for surface waters (*open symbol*) and groundwaters (*filled symbol*) for the December sampling campaign. The diagram also includes standard compositions for atmospheric (i.e., rainwater, At), lithrotropic (i.e., Ca-rich freshwater, Li) and thalassotrophic (i.e., seawater, Th) related waters

an important factor controlling water composition, an interpretation that is consistent with the overwhelming dominance of igneous rocks and, therefore, igneous rock-derived clastic sediments in the basin.

The Van Wirdum diagram (Fig. 6) gives a complementary insight. This type of diagram relates the ionic ratio (IR = $[Ca^{2+}]/([Ca^{2+}] + [Cl^{-}]$, with concentrations expressed in meq/L) vs. the electrical conductivity (EC) of the water samples (Birke et al. 2010; Tanaskovic et al. 2012). Whereas the EC is a measure of salinity, the IR can be seen as a measure of the prevalence of Ca^{2+} among the cations and Cl^{-} among the anions. Based on the position in the diagram, water samples can be classified considering three reference water types from the hydrological cycle as atmocline (At, i.e., rainwater), lithocline (Li, i.e., calcium rich fresh water), thassocline (Th, i.e., seawater) or anything in between. Figure 6 shows that most surface waters and groundwaters plot between these three end members, but especially in an imaginary line between the Li and Th types (although closer to Li). Actually, those samples that lie closest to the seawater end member are those of the lower part of the study area, near the basin outlet (i.e., L7, L8, L9, L10), which should be more influenced by oceanic aerosols (Graedel and Keene 1996). However, the local geology of that particular area, which includes the near surface Cenozoic marine terraces (Thomas 1967), is most likely the main cause of the chemical imprint of the waters. Again, no major differences were found between the samples of both campaigns.

Oxygen and hydrogen isotopes

Figure 7 shows the isotope signature of surface waters and groundwater in the study area considering the December

Table 2 Selected ionic ratios for surface water and groundwater in the area of study for both sampling campaigns, and expected values as described by Xiao et al. (2012) for carbonate weathering and silicate weathering controlled processes

Ionic ratio	Water component	Carbonate weathering	Silicate weathering	April campaign	December campaign
Ca^{2+}/Na^{+}	Surface water	50	0.35	0.68	0.84
	Groundwater			0.56	0.63
Mg^{2+}/Na^{+}	Surface water	10	0.24	0.39	0.41
	Groundwater			0.34	0.36
HCO_3^{-}/Na^{+}	Surface water	120	2	1.18	1.40
	Groundwater			1.22	1.29

sampling campaign, as well as the local meteoric line and the global water meteoric line.

Regarding the precipitation data, it must be acknowledged that 2 years is a rather short period and therefore the analysis and interpretation derived from this data must be made with caution. However, at the same time, it was, to the best of our knowledge, the only available local information of precipitation isotopic composition for the study area, and as such, this work represents a valuable contribution and baseline for further developments and application of these tools in North-Central Chile.

First, the isotopic composition of the precipitation exhibits a rather stable behavior for both rainfall-collecting seasons. Given that the local meteoric water line was similar for both years (i.e., $\delta^2H = 8.8\delta^{18}O + 17$ and $\delta^2H = 9.0\delta^{18}O + 20.12$ for 2009 and 2010, respectively, which $R^2 = 0.99$ in both cases), a weighted average local meteoric water line was determined ($\delta^2H = 8.9\delta^{18}O + 18.7$). Moreover, our results are in agreement, in particular regarding the slope of the meteoric line, with results described by Hoke et al. (2013) for the sub-tropical eastern flanks of South-Central Andes (33°–35°S). The intercept

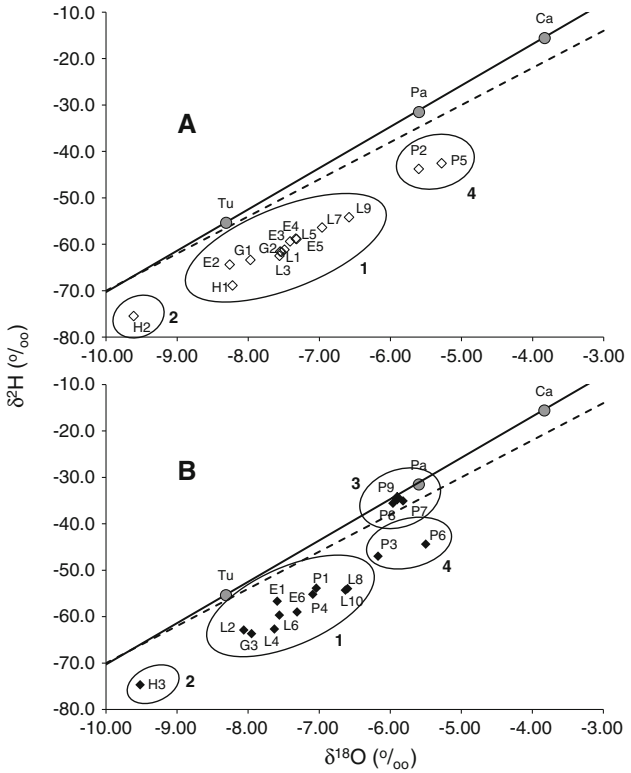

Fig. 7 Plot of $\delta^{18}O$ vs. δ^2H values of surface waters (**a**, *open symbol*) and groundwater (**b**, *filled symbols*) for the December sampling campaign. Also included are the local meteoric water line (*solid line*), the global meteoric line (*segmented line*) and the weighted mean isotopic composition of the precipitation for the Carretera (Ca), La Paloma (Pa) and Tulahuén (Tu) stations

differences in the meteoric lines may be attributed to different sources of atmospheric moisture. Evaporation from surface water creates vapor masses with isotopic contents that plot above the global meteoric water line (Clark and Fritz 1997). This can be the case of the study area because of the existence of three large dams where water is affected by evaporation. The role of this evaporation effect has been observed in precipitation in the Eastern Mediterranean region (Gat and Carmi 1970) and in condensed coastal fogs in Kenya (Ingraham and Matthews 1988).

Second, there is a clear altitude effect in the isotopic composition of the precipitation, i.e., $\delta^{18}O = -0.0053z$ (m) -3.1381 ($r^2 = 0.91$), considering the two years of data. The altitude effect has been previously documented in the Central part of the country where precipitation changed from $\delta^{18}O$ values around -5.5 ‰ on the coast to $\delta^{18}O$ values around -19 ‰ at 3,500 masl (Rozanski et al. 1993). A similar pattern have been reported in the Elqui River valley, located 80 km to the north of the study area, where the isotopic composition of water changes from $\delta^{18}O$ values of around -6 ‰ in the coastal areas to $\delta^{18}O$ values around -16 ‰ in the high mountains (Strauch et al. 2006).

Considering the isotopic signature of both surface waters and groundwater samples, these data showed that throughout the study area their isotopic composition, with the exception of the Punitaqui springs, do not correspond to that of local rainfall. They are characterized by depleted isotopic signatures when compared to the rainfall at La Paloma (Fig. 7). The other pattern observed in surface water and groundwater, excepting the Punitaqui springs, is that they plotted below the meteoric water, which is a typical pattern for water affected by evaporation. Thus, it is possible to infer that the water source for surface water and groundwater is heavily controlled by rainfall-runoff processes occurring in the upper parts of the basin, upstream of the reservoirs (Recoleta and La Paloma Dams). Water is then affected by evaporation in the dams, and is later conducted by the Grande, Hurtado, and Limarí rivers as well as by irrigation channels, diverting water from these rivers and dams, and thus distributed throughout the area of study, with further evaporation occurring in the irrigated areas and along the river's course. The effect of irrigation water in groundwater has been previously documented using isotopic tools in the Nile River Valley (El Bakri et al. 1992) and in the Central part of Chile (Fernández et al. 2013).

The effect of evaporation is clearly observed in the water representing the dams (G1 and H1). The deuterium excess (d-excess) is frequently used to document the role of evaporation (Strauch et al. 2006; Carreira et al. 2011). The values for the d-excess, for the dam water showed values always less than 10, which are values representative of evaporated waters. However, the other water samples, L1,

L3, L5, L7 and L8, representing the Limarí River, after the intersection between the Grande and Hurtado Rivers, does not follow a clear isotopic pattern associated to only evaporation along the river course using as a water source the dam water (Fig. 7). A similar pattern is observed for the surface water in the Ingenio Creek basin (E2, E3, E4 and E5). For evaporation from an open water body, a slope of 5.0 is expected for the evaporation line at a relative humidity of 70 %, which is the average value for the study area (Clark and Fritz 1997). The regression lines for the Limarí River and Ingenio Creek are: $\delta^2H = -6.7\delta^{18}O - 10.4$, and $\delta^2H = -7.1\delta^{18}O - 7.4$, respectively. Then, the slopes are higher than expected for evaporation only.

The groundwater follows the same pattern than the surface water. They plotted below the meteoric water line and in most the cases, the isotopic composition of the groundwater is slightly depleted or similar than the isotopic composition of the surface water in areas where both samples were collected in the same area. This pattern shows a clear link between groundwater and surface water in the study area. One clear example is the data collected in groundwater and surface water in the Punitaqui Basin. The isotopic composition of the local recharge is represented by the isotope data collected for the Punitaqui springs which are characterized by values of −35 ‰ and −5.6 ‰ for δ^2H and $\delta^{18}O$, respectively (Table 1). Similar isotope values have been reported in groundwater near coastal areas in the Romeral basin located near the city of La Serena (Squeo et al. 2006), which is under the same precipitation regime as the study area. In case of the surface water of the Punitaqui creek (P2, P5), they are characterized by values around −46 and −6.0 for δ^2H and $\delta^{18}O$, respectively. These data plotted also below the meteoric water line (Fig. 7) and indicated that the surface water is not originated from local recharge. The surface water seems to be part of the isotopic pattern observed in the groundwater (P4, P6 and P6). The source of recharge to the groundwater is the irrigation channels that bring water from the La Paloma reservoir and the Grande River into the Punitaqui area. The groundwater at P1 with values of δ^2H around −55 ‰ and $\delta^{18}O$ of −7.0 ‰ is representative of this type of water.

There are some exceptions to this general pattern, represented by the samples collected downstream from the Recoleta dam, i.e., H2 (surface water) and H3 (groundwater), which exhibit a more depleted isotopic signature than the Recoleta reservoir (H1) and moderately higher salinity (Fig. 8). This pattern, repeated in both sampling campaigns, seems to point toward the fact that these waters do not correspond only to infiltration-exfiltration processes from the upstream, neighboring Recoleta reservoir but also to waters that precipitate at higher elevations (ca. 1,100 masl) in the Hurtado River sub-basin, which then become part of the groundwater flow system controlled by deep rock fractures and discharge at the H2 and H3 location. The other interesting isotopic pattern is observed in the surface and groundwater in the Ingenio Creek. Their isotope values are much lower than the expected values for the local precipitation indicating that the Ingenio Creek is feed by leakage of the Recoleta Dam.

The role of evaporation can be further evaluated exploring the relationship between $\delta^{18}O$ values and salinity represented by conductivity values (Fig. 8). Considering the data collected in the Limari river, it can be observed that a significant increase in conductivity values from ∼500 to 3,500 µS/cm is observed between the high (G1, H1) and lower part of the basin (L8). A similar pattern is observed in the Ingenio Creek watershed (E2–E5). However, a relative small change is observed in the $\delta^{18}O$ values, from ∼−8 to −7 ‰ in case of the Limarí River and the Ingenio Creek. A similar pattern is observed in the groundwater which is a reflection of its link with the surface water. The water that showed a relative greater evaporation effect are those samples in the Punitaqui area, which showed an increase in salinity from ∼500 µS/cm (taking into account the source of water to this area are the La Paloma dam and the Grand River) to values over 2,500 µS/cm. This pattern is accompanied by a change in $\delta^{18}O$ values from ∼−8 to −5 ‰, which is larger than the change observed in Limarí and Ingenio areas associated to a rather similar increase in salinity. These observations confirmed that evaporation does not play a major role in the chemistry of the surface and groundwater in the Limarí and Ingenio basins but it is more relevant in the Punitaqui area.

Sulfur isotopes

Figure 9 displays the sulphate concentrations and $\delta^{34}S$ signatures on surface waters and groundwater from the

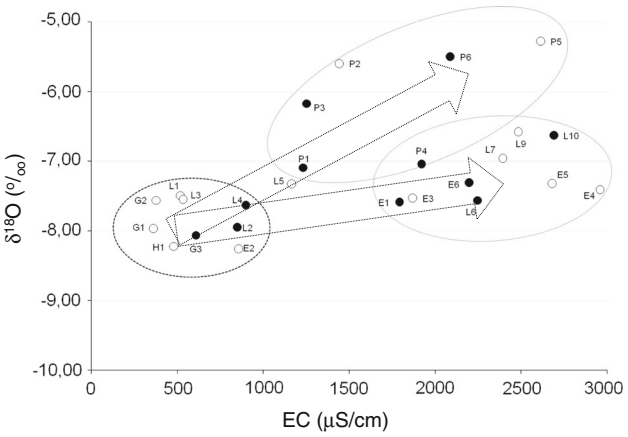

Fig. 8 Electrical conductivity (EC) vs. ^{18}O

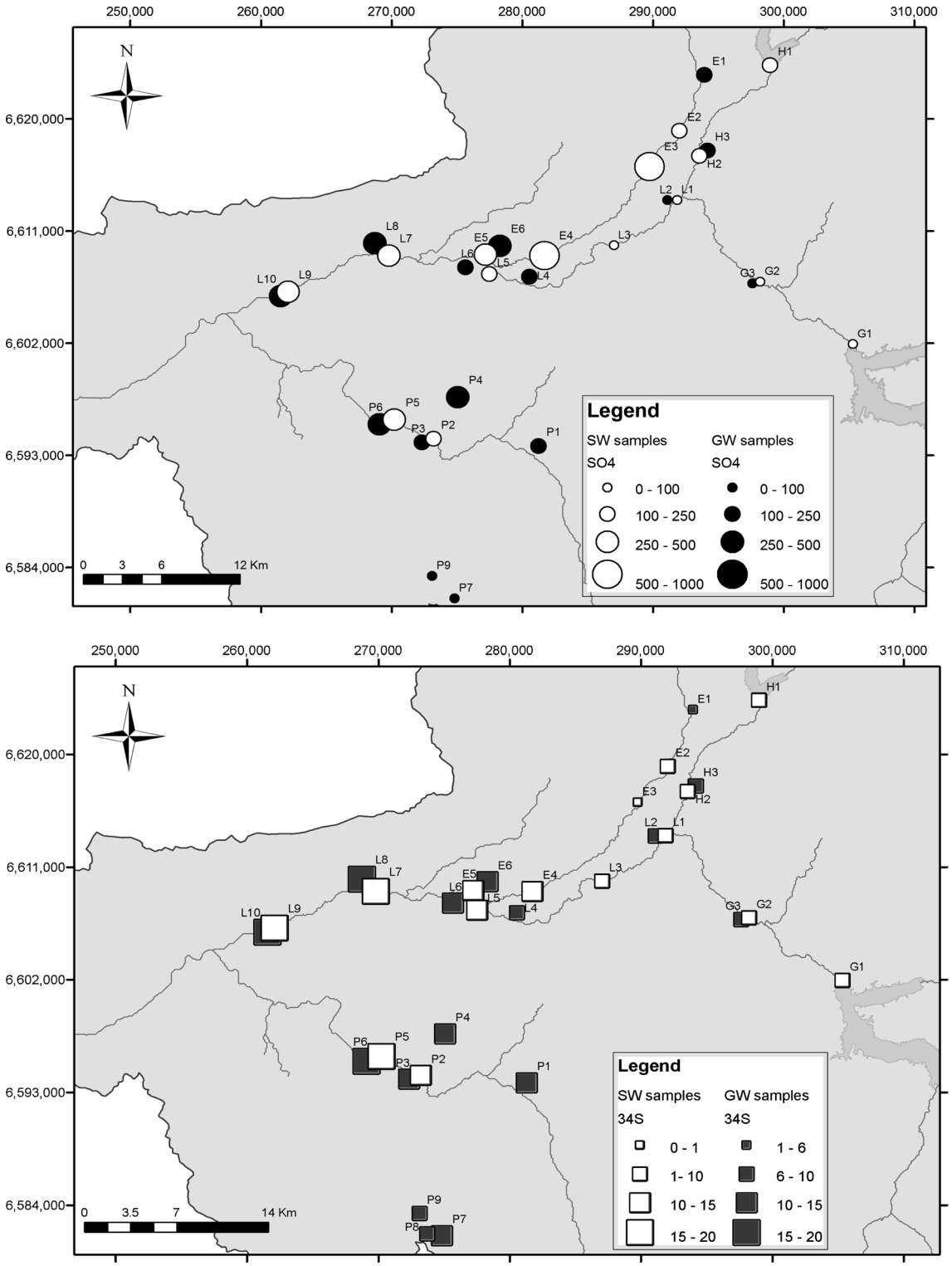

Fig. 9 Sulfate concentrations (mg/L) (*top panel*) and $\delta^{34}S$ (‰) (*bottom panel*) in surface waters (*white symbol*) and groundwater (*black symbol*) in the study area

December sampling campaign. The ^{34}S data provide information about the sources of sulphate associated with the increase in SO_4^{2-} concentrations from East to West. The sulphate in the upper parts of the study area, in the water reservoirs and immediately downstream from them (Hurtado and Grande rivers, and the initial reach of the

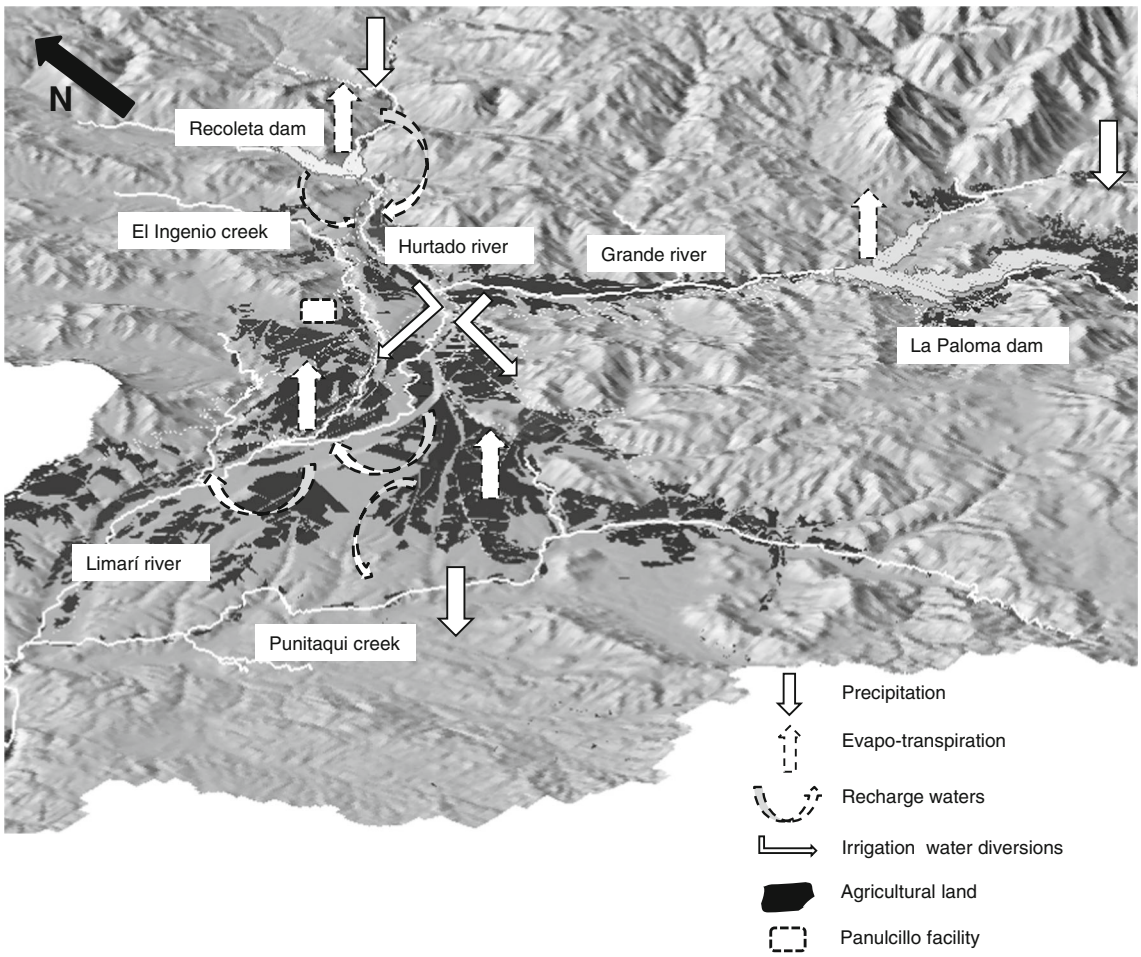

Fig. 10 Conceptual model of the geo-hydrological relations in the study area (main irrigation channels are depicted as *segmented white lines*)

Limarí River) is characterized by $\delta^{34}S$ values ranging between 4 and 7 ‰, which is a typical range for igneous sources. Thus, these values represent water-altered rocks interactions (hydrothermal sulphate plus SO_4^{2-} derived from sulphide minerals oxidation), mostly occurring upstream of the Recoleta and Paloma dams. This is consistent with the information derived from the Gibbs diagram and the ion ratios described before. As water flows downstream through the Limarí River, sulphate $\delta^{34}S$ values increase, reaching a value of around 16 ‰. This pattern is also accompanied by an increase in sulphate concentration, which is evidence of additional sources of sulphate in waters, most likely from dissolution of saline evaporates (e.g. gypsum) existing in the marine terraces west of Ovalle. Indeed, $\delta^{34}S$ values around 20 ‰ could be expected from marine evaporates in areas near the Ocean (Pu et al. 2013). The only exception to this general pattern corresponds to the sampling point E3, located immediately downstream from the currently closed Panulcillo mining facility, where $\delta^{34}S$ data show a value of 0.8 ‰, an isotopic signature most likely related with hydrothermal, magmatic-related sulphur, present in the copper ore mineral formerly processed at the Panulcillo facility. Furthermore, H_2SO_4 used by this facility was obtained from Chilean copper smelters, which also processed magmatic-related sulphur ore minerals. This location is also characterized by the highest sulphate concentration in the study area (between 700 and 800 mg/l). The trend toward more enriched $\delta^{34}S$ values from 0.8 ‰ (E3) to 14.6 (E4) and 13.1 ‰ (E5) along the Ingenio Creek, similarly to the Limarí River, showed also the influence of marine evaporates in the chemistry of these waters.

Conceptual hydrological-hydrochemical model for the study area

Based on the analysis of the chemical and isotopic data and the water usage in the study area, a basic conceptual model of the geo-hydrological behavior of the area was developed (Fig. 10). It considers local precipitation to be of low importance in the sub-basin in terms of surface flow and groundwater recharge. It is proposed that the hydrology

and hydrogeology in the study area are controlled by water stored in the reservoirs (La Paloma and Recoleta), diverted through channels as well as from the rivers, used in irrigation in the agricultural lands, and returning to the stream as irrigation excess water (surface runoff) and recharge and discharge of shallow groundwater (return flow). In terms of water chemistry, the following sources are relevant: (a) Igneous and volcanic-sedimentary rocks. This includes hydrothermal alteration zones and rock outcrops affected by hydrothermal alteration and ARD, mainly on the Andean heights drained by the tributary rivers, and weathered granitoid outcrops. Both sources contribute Na^+, K^+, Ca^{2+}, Mg^{2+}; (b) Partly marine Pliocene–Quaternary terraces, contributing Ca^{2+}, Na^+, SO_4^{2-}, and Cl^-; (c) Vegetal matter decay that determines the generation of HCO_3^-; (d) The atmosphere, that transfers NaCl aerosols from the Pacific Ocean towards inland areas; (e) Mining-metallurgical activities at El Ingenio creek, mainly for SO_4 from the leaching of Cu minerals.

The study showed that surface waters and shallow groundwater are actively connected, which is verified by the similar chemical and isotopic compositions of both components, especially in neighboring sampling locations. The only exception corresponds to the non-irrigated part of the Punitaqui basin (spring samples at Rinconada de Punitaqui), where local precipitation is the only source of the scarce surface water flows and limited groundwater resources. Finally, the historical mineral processing activities of the former Panulcillo facility still have an important, but rather local effect on water composition, as observed in the El Ingenio Creek.

Conclusions

In general, surface and ground water follow the same chemical and isotopic pattern through the study area, indicating an active level of interaction between these water compartments. In chemical terms, these waters are mostly classified as Ca–HCO_3 in the upper part of the study area, changing to Ca–Na–Cl towards the lower part of the basin.

The results obtained for both surface and ground waters indicate a general trend of increasing values in EC, TDS, Ca^{2+}, Mg^{2+}, Na^+, K^+, Cl^-, and SO_4^{2-} from upstream to downstream in the study area. Considering each of the five sub-basins in this study, it can be observed that the Grande and Hurtado rivers were characterized by the lowest ion concentrations. The higher salinity waters were observed in El Ingenio Creek due to the pollution effect of the old Panulcillo facility (reflected in the high level of SO_4^{2-}) and in the lower part of the Limarí River due to the contribution of salts from marine sediments.

Thus, based on chemical ratios and isotope data, the main processes and factors that determine the chemical characteristics of the waters in the complete study area are: (a) the effect of recharge of surface water used for irrigation in the agricultural areas and return flow to rivers (supported by the stable isotope data in water), (b) input of sulfate solutions into the waters of El Ingenio Creek associated with a former minerals processing facility, (c) water–rock interaction processes (silicate weathering), and (d) input of solutes from marine terraces at the El Ingenio and Punitaqui creeks as well as the last reaches of the Limarí River that translate into increased salt concentrations of the waters. Moreover, at the outlet of the reservoirs, the S-isotopic signal is representative of igneous rocks that exist upstream of the dams. El Ingenio Creek has the lowest value of $\delta^{34}S$, and the highest SO_4^{2-} concentrations, which shows that the latter comes especially from the former processing activities performed at Panulcillo. In the lower parts of El Ingenio Creek and the Limarí basin, the $\delta^{34}S$ values and the chemical composition are indicative of the contribution from marine sedimentary deposits.

Considering the water stable isotope data, the observed patterns correspond to a combination of evaporation of water in reservoirs, water distribution from the reservoirs through the main course (river) and irrigation canals, evaporation of water in the soil (soil water and irrigation) and along the river course, and, to a lesser degree, input from local precipitation. Groundwater discharge associated with higher altitude recharge areas than the rest of the water in the study area was also documented by the isotope data in the Hurtado River. It is important to note that in general both surface water and groundwater showed similar isotopic patterns, which is an indication that they are interconnected. This strengthens the hypothesis postulated based on the chemical data of an active interaction between these water compartments. It is important to highlight that the use of the river water is regulated by an irrigation council formed by member of the agriculture community but not the use of groundwater. Due to extreme drought conditions during the last 5 years in the study region, an increasing pressure on groundwater use is expected, therefore based on the results of this study, a more comprehensive study on groundwater–surface water interaction using hydrogeological and hydrological tools is warranted in the study area.

Acknowledgments This work was funded by the International Atomic Energy Agency (AIEA) through the Technical Cooperation Project CHI 8029, and DIULS CD093401 (Research Office of the University of La Serena), and was conducted as part of the Water Resources and Environment Program (PRHIMA) of the Department of Mining Engineering of the University of La Serena. The authors are much indebted to the Dirección General de Aguas (DGA, Ministerio de Obras Públicas) and to Carabineros de Chile for allowing

the installation of rainfall collectors within their facilities, as well as to the APR's committees for allowing sampling of their wells. The paper benefited from the comments of two anonymous reviewers.

References

Aggarwal PK, Araguas L, Garner WA, Groeninig M, Kulkarni K (2007) Introduction to water sampling analysis for isotope hydrology. Water Resources Programme—IAEA. http://www-naweb.iaea.org/napc/ih/documents/other/Sampling%20booklet%20web.pdf. Accessed December 2009

Alvarez P, Oyarzún R (2006) Interacción río-acuífero en zonas áridas: contexto legal y análisis de casos (River−aquifer interaction: legal context and study cases). VIII Congreso Latino Americano de hidrología subterránea (ALSHUD), Asunción, Paraguay

Baskaran S, Ransley T, Brodie RS, Baker P (2009) Investigating groundwater–river interactions using environmental tracers. Aust J Earth Sci 56(1):13–19

Birke M, Rauch U, Harazim B, Lorenz H, Glatte W (2010) Major and trace elements in German bottled water, their regional distribution, and accordance with national and international standards. J Geochem Explor 107:245–271

Carreira PM, Marques JM, Espinha J, Chaminé HI, Fonseca PE, Monteiro F, Moura RM, Carvalho JM (2011) Defining the dynamics of groundwater in Serra da Estrela mountain area, Central Portugal: and isotopic and hydrogeochemical approach. Hydrogeol J 19:117–131

Clark I, Fritz P (1997) Environmental isotopes in hydrogeology. Lewis, New York, p 328

Clesceri LS, Greenberg AE, Eaton AD (1999) Standard methods for the examination of water and wastewater, 20th edn. American Public Health Association, American Water Works Association, Water Environmental Federation, Washington

CONAMA (Comisión Nacional del Medio Ambiente) (2006) Estudio de la variabilidad climática en Chile para el siglo XXI (Study of the climate variability in Chile at the XXI century). Comisión Nacional del Medio Ambiente, Santiago

Dansgaard W (1964) Stable isotopes in precipitation. Tellus XVI 4:436–468

Demirel Z, Güller C (2006) Hydrogeochemical evolution of groundwater in a Mediterranean coastal aquifer, Mersin-Erdemli basin (Turkey) Environ Geol 49:477–487

DGA (Dirección General de Aguas) (2004) Diagnóstico y clasificación de los cursos y cuerpos de agua según objetivos de calidad. Cuenca del Río Limarí (Diagnosis and classification of water bodies based on water quality objectives. Limarí river basin). Dirección General de Aguas, CADE IDEPE Consultores

DGA (Dirección General de Aguas) (2008) Evaluación de los recursos hídricos subterráneos en la cuenca del rio Limarí (Groundwater resources assessment in the Limarí river basin). Informe Técnico N° 268, Dirección General de Aguas

Drever JI (1997) The geochemistry of natural waters. Surface and groundwater environments, 3rd edn. Prentice Hall, New Jersey, p 436

El Bakri A, Tantawi A, Blavoux B, and Dray M (1992) Sources of water recharge identified by isotopes in the ElMynya Governate (Nile Valley, Middle Egypt). In: Isotope techniques in water resources development 1991, IAEA symposium 319, Vienna, pp 643–645

Emparán C, Pineda G (2006) Geología del Area Andacollo-Puerto Aldea, Región de Coquimbo (Geology of the Andacollo-Puerto Aldea are, Coquimbo Region). Servicio Nacional de Geología y Minería, Carta Geológica N° 96, Santiago. Carta 1:100,000

Espejo L, Kretschmer N, Oyarzún J, Meza F, Núñez J, Maturana H, Soto G, Oyarzo P, Garrido M, Suckel F, Amézaga J, Oyarzún R (2011) Application of water quality indices and analysis of the surface water quality monitoring network in semiarid North-Central Chile. Environ Monit Assess 184(9):5571–5588

Espinoza MC (2005) Vulnerabilidad de los acuíferos en los ríos Limarí y Maule mediante las metodologías GOD y BGR (Aquifer vulnerability in the Limarí and Maule river basins base don the GOD and BGR methodologies). Memoria de Título, Departamento de Geología, Facultad de Ciencias Físicas y Matemáticas, Universidad de Chile

Fernández E, Grilli A, Aravena R, Alvarez D (2013) Determinación de la presencia de nitrógeno de diversas fuentes en aguas subterráneas en un acuífero agrícola (Assessment on the presence of nitrate from several sources in groundwater of a rural aquifer). XX Congreso de Ingenieria Sanitaria y Ambiental, Aidis-Chile

Freeze AL, Cherry JA (1979) Groundwater. Prentice Hall, New Jersey, p 604

Friedman I, Smith GI, Gleason JD, Warden A, Harris JM (1992) Stable isotope composition of waters inSoutheastern California. 1. Modern Precipitation. J Geophys Res 97:5795–5812

Gaillardet J, Dupré B, Lovat P, Allegre CJ (1999) Global silicate weathering and CO_2 consumption rates deduced from the chemistry of large rivers. Chem Geol 159:3–30

Gat JR, Carmi I (1970) Evolution of the isotopic composition of atmospheric waters in the Mediterranean Sea area. J Geophys Res 75:3039–3048

Graedel TE, Keene WC (1996) The budget and cycle of Earth's natural chlorine. Pure Appl Chem 68:1689–1697

Guay BE, Eastoe CJ, Basset R, Long A (2006) Identifying sources of groundwater in the lower Colorado River valley, USA, with δ18O, δD, and 3H: implications for river water accounting. Hydrogeol J 14:146–158

Güller C, Thyne G, McGray JE, Turner AK (2002) Evaluation of graphical and multivariate statistical methods for classification of water chemistry data. Hydrogeol J 10:455–474

Herczeg AL, Leaney FW (2011) Review: environmental tracers in arid-zone hydrology. Hydrogeol J 19:17–29

Hoke GD, Aranibar JN, Viale M, Araneo DC, Llano C (2013) Seasonal moisture sources and the isotopic composition of precipitation, rivers and carbonates across the Andes at 32.5–35.5°S. Geochem Geophy Geosy 14:962–978

INE (Instituto Nacional de Estadísticas) (2007) VII Censo nacional agropecuario y forestal (VII Agricultural and forestry census). Instituto Nacional de Estadísticas. http://www.censoagropecuario.cl/noticias/08/6/10062008.html. Accessed 12 May 12 2010

Ingraham NL, Matthews RA (1988) Fog drip as a source of groundwater recharge in northern Kenya. Water Resour Res 24:1406–1410

López-Escobar L, Frey FA, Oyarzún J (1979) Geochemical characteristics of central Chile (33°–34°S) granitoids. Contrib Mineral Petrol 70:439–450

Maliva R, Missimer T (2012) Arid lands, water evaluation and management. Springer, Berlin. doi:10.1007/978-3-642-29104-3_2

Matter JM, Waber NH, Loew S, Matter A (2005) Recharge areas and geochemical evolution of groundwater in an alluvial aquifer system in the Sultanate of Oman. Hydrogeol J 14:203–224

Mook WG (2001) Environmental isotopes in the hydrological cycle. Principles and applications IHP-V. Technical documents in Hydrology, N° 39. UNESCO-IAEA

Morrison J (1997) Inorganic oxygen isotope analysis by EA-Pyrolysis-IRMS. IV Canadian Continuous Flow, IRMS Conference

Morrison J, Fallick T, Donelly T, Leossen M, St. Jean G, Drimmie R J (1996) $\delta^{34}S$ Measurements of standards from several laboratories by continuous flow isotope ratio mass spectrometry (CF-IRMS). Micromass UK Ltd. Technical Note TN 309

Oyarzún J, Levi B, Nystrom JO (1993) A within-plate geochemical signature and continental margin setting for the Mesozoic-Cenozoic lavas of central Chile. Second ISAG, Oxford (UK), pp 419–422. http://horizon.documentation.ird.fr/exl-doc/pleins_textes/pleins_textes_6/colloques2/38461.pdf. Accessed 28 February 2013

Oyarzún R, Arumí JL, Alvarez P, Rivera D (2008) Water use in the Chilean agriculture: current situation and areas for research development. In: Sorensen ML (ed) Agricultural water management trends. Nova Publishers, New York, pp 213–236

Pu J, Yuan D, Zhang C, Zhao H (2013) Hydrogeochemistry and possible sulfate sources in karst groundwater in Chongquing, China. Environ Earth Sci 68(1):159–168

Rozanski K, Araguas-Aragua L, Gonfiantini R (1993) Isotopic patterns in modern global precipitation. In: Swart PK, Lohmann KC, McKenzie J, Savin S (eds) Climate change in continental isotopic records. In: Geophysical monograph, vol 78. American Geophysical Union, Washington, pp 1–36

SERPLAC, DGA, ONU, CORFO (1979) Hidrogeología de la cuenca del río Limarí. Investigación de recursos hidráulicos en la IV región (Limarí basin hydrogeology. Research on hydraulic resources in the Region IV). Proyecto CHI-535

Shi JA, Wang Q, Chen GJ, Wang GY, Zhang ZN (2001) Isotopic geochemistry of the groundwater systems in arid and semiarid areas and its significance: a case study in Shiyang River basin, Gansu province, northwest China. Environ Geol 40:557–565

Simmers I (2003) Hydrological processes and water resources management. In: Simmers I (ed) Understanding water in a dry environment. Hydrological processes in arid and semi-arid zones. International Association of Hydrogeologists. A. A. Balkema, Rotterdam, pp 1–14

Souvignet M, Gaesse H, Ribbe L, Kretschmer N, Oyarzún R (2010) Statistical downscaling of precipitation and temperature in North-Central Chile: an assessment of possible climate change impacts in an arid Andean watershed. Hydrolog Sci J 55(1):41–57

Squeo FA, Aravena R, Aguirre E, Pollastri A, Jorquera CB, Ehleringer JR (2006) Groundwater dynamics in a coastal aquifer in North-central Chile: implications for groundwater recharge in an arid ecosystem. J Arid Environ 67:240–254

Strauch G, Oyarzún J, Fiebig-Wittmaack M, González E, Weise S (2006) Contributions of the different water sources to the Elqui river runoff (northern Chile) evaluated by H/O isotopes. Isot Environ Health S 42(3):303–322

Strauch G, Oyarzún R, Reinstorf F, Oyarzún J, Schirmer M, Knöller K (2009) Interactions of water components in the semi-arid Huasco and Limarí river basins, North Central Chile. Adv Geosci 22:51–57

Tanaskovic I, Golobocanin D, Miljevic N (2012) Multivariate statistical analysis of hydrochemical and radiological data of Serbian spa waters. J Geochem Explor 112:226–234

Thomas H (1967) Geología de la Hoja Ovalle, Provincia de Coquimbo (Geology of the Ovalle Sheet, Coquimbo Region). Instituto de Investigaciones Geológicas, Boletín N° 23. Santiago, 58 pp and geologic map 1:250,000

Thyne G, Güller C, Poeter E (2004) Sequential analysis of hydrochemical data for watershed characterization. Ground Water 42:711–723

Xiao J, Jin Z, Zhang F, Wang J (2012) Major ion geochemistry of shallow groundwater in the Quinghai lake catchment. NE Quinghai-Tibet Plateau. Environ Earth Sci 67(5):1331–1344

Yang L, Song X, Zhang Y, Yuan R, Ma Y, Han D, Bu H (2012) A hydrochemical framework and water quality assessment of river water in the upper reaches of the Huai River Basin. China. Environ Earth Sci 67(7):2141–2153

Yin L, Hou G, Su X, Wang D, Dong J, Hao Y, Wang X (2011) Isotopes (δD and $\delta D^{18}O$) in precipitation, groundwater and surface water in the Ordos Plateau, China: implications with respect to groundwater recharge and circulation. Hydrogeol J 19:429–443